doi:10.1111/j.1558-5646.2011.01441.x

INDEPENDENT AXES OF GENETIC VARIATION AND PARALLEL EVOLUTIONARY DIVERGENCE OF OPERCLE BONE SHAPE IN THREESPINE STICKLEBACK

Charles B. Kimmel,[1,2] William A. Cresko,[3,4] Patrick C. Phillips,[3] Bonnie Ullmann,[1] Mark Currey,[3] Frank von Hippel,[5] Bjarni K. Kristjánsson,[6] Ofer Gelmond,[5] and Katrina McGuigan,[3,7]

[1]*Institute of Neuroscience, University of Oregon, Eugene Oregon 97403*

[2]*Email: kimmel@uoneuro.uoregon.edu*

[3]*Institute of Ecology and Evolution, University of Oregon, Eugene Oregon 97403*

[4]*Email: wcresko@uoregon.edu*

[5]*Department of Biological Sciences, University of Alaska Anchorage, 3211 Providence Dr., Anchorage, Alaska 99508*

[6]*Holar University College, Háeyri 1, 550 Sauöárkrókur, Iceland*

[7]*School of Biological Sciences, The University of Queensland, QLD 4072, Australia*

Received January 20, 2011
Accepted July 22, 2011
Data Archived: Dryad doi:10.5061/dryad.540k5

Evolution of similar phenotypes in independent populations is often taken as evidence of adaptation to the same fitness optimum. However, the genetic architecture of traits might cause evolution to proceed more often toward particular phenotypes, and less often toward others, independently of the adaptive value of the traits. Freshwater populations of Alaskan threespine stickleback have repeatedly evolved the same distinctive opercle shape after divergence from an oceanic ancestor. Here we demonstrate that this pattern of parallel evolution is widespread, distinguishing oceanic and freshwater populations across the Pacific Coast of North America and Iceland. We test whether this parallel evolution reflects genetic bias by estimating the additive genetic variance–covariance matrix (G) of opercle shape in an Alaskan oceanic (putative ancestral) population. We find significant additive genetic variance for opercle shape and that G has the potential to be biasing, because of the existence of regions of phenotypic space with low additive genetic variation. However, evolution did not occur along major eigenvectors of G, rather it occurred repeatedly in the same directions of high evolvability. We conclude that the parallel opercle evolution is most likely due to selection during adaptation to freshwater habitats, rather than due to biasing effects of opercle genetic architecture.

KEY WORDS: **Craniofacial, G matrix, *Gasterosteus aculeatus*, genetic basis of traits, genetic bias, genetic constraint, microevolution, quantitative genetics.**

A general appreciation exists in evolutionary biology that certain architectures of genetic variation can bias, constrain, or channel evolution (Dickerson 1955; Lande 1979; Cheverud 1984; Arnold 1992; Beldade et al. 2002). Evolution is expected to proceed along what have been termed as "evolutionary lines of least resistance" (Stebbins 1974), which are regions of phenotypic space that contain the most genetic variation. Quantitative genetic studies of bias have focused on the major eigenvector of the genetic (co)variance matrix **G**, otherwise known as $\boldsymbol{g}_{max}$, which represents the linear combination of traits with the greatest potential for evolution

(evolvability; Hansen and Houle 2008). An argument can therefore be made that $\boldsymbol{g}_{max}$ captures a significant proportion of the biasing effects of genetic architecture. In addition, $\boldsymbol{g}_{max}$ captures the single greatest axis of pleiotropic variation in a suite of measured traits, and it therefore might be expected to bias the direction of phenotypic evolution if it also captures much of the pleiotropic covariation of the measured traits and fitness (McGuigan et al. 2010b).

Despite the intuitive simplicity of the hypothesis that $\boldsymbol{g}_{max}$ is a major biasing genetic factor in evolution, empirical support for this proposition has been inconsistent. In a highly influential paper, Schluter (1996) tested the hypothesis that multivariate phenotypic evolution is biased toward the direction described by $\boldsymbol{g}_{max}$. He presented results from a wide range of taxa (birds, fish, and mice) supporting the proposition that $\boldsymbol{g}_{max}$ biases phenotypic evolution, and that this bias decays over time. However, subsequent studies with other taxa have yielded mixed results (Begin and Roff 2003; McGuigan et al. 2005; Chenoweth et al. 2010). Similarly, studies of whether evolution has been biased by the phenotypic axis associated with greatest variation have yielded inconsistent support (Merilä and Björklund 1999; Badyaev and Hill 2000; Berner et al. 2010).

Recently, there has been a growing appreciation that the relationship between $\boldsymbol{g}_{max}$ and biased evolution is more nuanced than previously thought, and that the entire structure of **G** must be considered in questions of evolutionary constraint. For example, the effect of $\boldsymbol{g}_{max}$ on the direction of phenotypic evolution will be influenced by the geometry of **G**. If $\boldsymbol{g}_{max}$ captures a large portion of the genetic variance (**G** is "ill-conditioned"), then $\boldsymbol{g}_{max}$ will strongly bias phenotypic evolution (Chenoweth et al. 2010) over longer timeframes (Jones et al. 2003). However, if genetic variation is relatively equally distributed among different trait combinations, then axes of genetic variation other than $\boldsymbol{g}_{max}$ may also be evolutionary lines of least resistance and associated with the direction of divergence. Therefore, the relative amounts of variation explained by the primary eigenvectors of **G** must be considered along with just $\boldsymbol{g}_{max}$. Relatively few studies have considered the association between genetic vectors other than $\boldsymbol{g}_{max}$ and the direction of phenotypic divergence, and these have also met with mixed results (Blows and Higgie 2003; Begin and Roff 2004; McGuigan et al. 2005; Chenoweth et al. 2010; Simonsen and Stinchcombe 2010).

The overall structure of **G** can affect the trajectory of phenotypic evolution in even more subtle ways than just the major axes of evolvability. A particular combination of traits may be evolutionarily very accessible because of a preponderance of genetic variation in those regions of phenotypic space, and other regions be inaccessible because of a lack of genetic variation in those regions of phenotypic space (Mezey and Houle 2005; Walsh and Blows 2009). This proposition has some empirical support (Hine and Blows 2006; McGuigan and Blows 2007). In a survey of five datasets, representing different taxa and traits, Kirkpatrick (2009) determined that even when a large number of traits were measured, the number of genetically independent trait combinations was less than two. Genetic constraints, in the form of prohibited regions of phenotypic space, are likely to be common. Therefore, the overall biasing effects of **G** can be thought of as constraining evolution to occur in directions associated with high evolvability (Hansen and Houle 2008), a hypothesis for which there is some support (Hansen and Houle 2008; Hansen and Voje 2011). This constraining effect will be particularly important if the evolutionarily important phenotypic variation condenses to a few (or one) genetic axes of variation.

The question of genetic bias is particularly relevant to studies of parallel or convergent evolution. The evolution of similar phenotypes in isolated populations and species has often been used as strong evidence for the action of natural selection (Endler 1986; Schluter 2000), particularly when the phenotypes are correlated with specific environmental variables (Endler 1986). However, the direction of phenotypic evolution might also be affected by the development and genetic architecture of the traits under selection, leading to a biased evolutionary trajectory that is dissociated from the fitness landscape (Lande and Arnold 1983; Price et al. 1993; Steppan et al. 2002). Natural evolutionary systems in which replicate populations, derived from a common ancestral stock, have independently evolved similar phenotypes are powerful tools in evolutionary biology. Threespine stickleback (*Gasterosteus aculeatus*) provide a textbook example of parallel phenotypic evolution (Cresko et al. 2004; Shapiro et al. 2004; Colosimo et al. 2005; Miller et al. 2007), and thus provide an excellent natural experiment with which to test whether genetic variance might have biased the direction of divergence (Bell and Foster 1994; Schluter 2000; Taylor and McPhail 2000; Cresko et al. 2007).

Stickleback are distributed holarctically in coastal regions of the northern hemisphere, where freshwater populations often represent relatively recent residents, colonizing new freshwater habitats after the retreat of glaciers from the last glacial maximum (often less than 14,000 years bp). Molecular population genetic data indicate that even geographically proximate freshwater populations can have independent evolutionary histories (Taylor et al. 1997; Thompson et al. 1997; Taylor and McPhail 2000; Hendry et al. 2002; Watanabe et al. 2003; McKinnon et al. 2004; Hohenlohe et al. 2010). Despite this independent evolution, many different freshwater populations have evolved phenotypes relatively similar to one another, and typically relatively dissimilar to the oceanic phenotype (Bell and Foster 1994; Schluter 2000; Taylor and McPhail 2000; Cresko et al. 2007). In many regions, the extant oceanic populations serve as compelling surrogates for the ancestral population that gave rise to the replicate freshwater lineages,

providing the opportunity for direct comparisons between the genetic architecture of traits in the ancestral oceanic population and the direction of evolution in derived freshwater populations.

One stickleback phenotype that has evolved in parallel among freshwater populations in South Central Alaska is the shape of the opercle bone (Kimmel et al. 2005, 2008; Arif et al. 2009). The opercle supports the cover of the gill chamber and functions in respiration and feeding. Near the surface of the body, and thus easily observed, the opercle arises early in development from a relatively simple primordium of osteoblasts and achieves the adult shape by stereotypical differential outgrowths of the separate edges of the bone (Kimmel et al. 2008, 2010). Molecular developmental studies of the opercle bone's evolution may be particularly fruitful. Studies encompassing several levels of biological organization—from the cellular underpinnings of opercle growth and morphogenesis to the ancestral genetic architecture and divergence among evolving populations in the shaping of the adult bone—can ultimately be synthesized to deeply understand the creation of ecologically important skeletal phenotypic variation.

Compared to a local oceanic population, the opercles of sticklebacks from freshwater lakes exhibit dilation–diminution (Kimmel et al. 2008; Arif et al. 2009), defined as an anterior–posterior stretching out, coupled with a dorsal–ventral compression of its shape (Fig. 1, arrows in B). This pattern of opercle shape variation in Alaskan stickleback is striking, but it remains to be determined if the pattern is general, or is specific to Alaska. Here, we test the hypothesis that the parallel divergence in opercle bone shape between oceanic and freshwater stickleback is a widespread phenomenon by examining populations from South Central Alaska, the site of earlier work, as well as from Middleton Island, Alaska, and from British Columbia, Oregon, and Iceland. We further test the hypothesis that the major axis of oceanic to freshwater divergence among the 22 populations assayed is associated with genetic variance in a putative ancestral stickleback population. We estimate this major axis of genetic variance through a large half-sibling quantitative genetic breeding design, implemented using individuals from Rabbit Slough, an Alaskan oceanic population. Molecular population genomic data support Rabbit Slough as a good surrogate for the ancestral population likely to have given rise to freshwater populations throughout the Cook Inlet Basin (Hohenlohe et al. 2010).

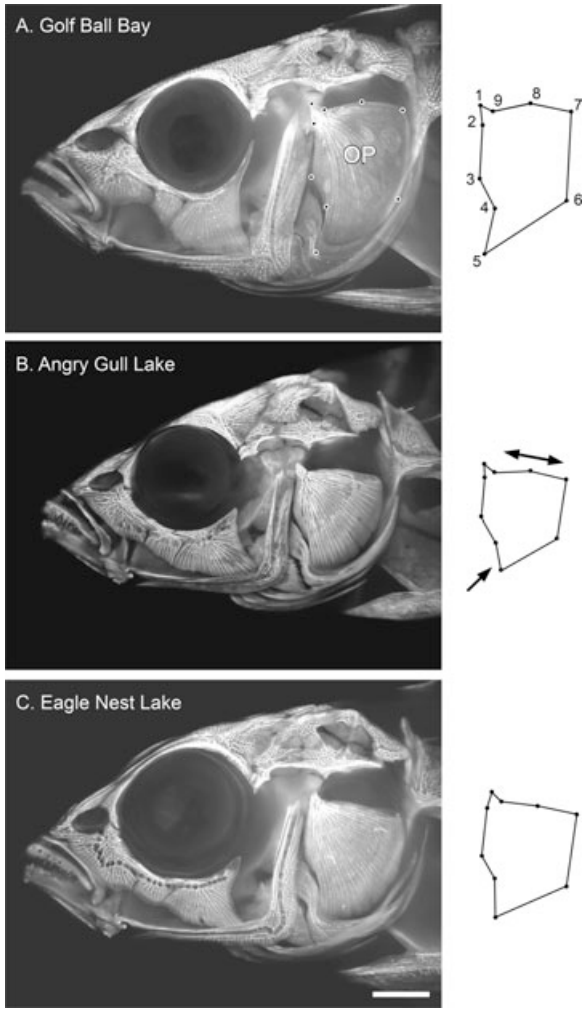

Figure 1. Opercle (OP) morphology has evolved rapidly (46 years) and in parallel in threespine sticklebacks. Alizarin Red stained Middleton Island fish imaged by epifluorescence. The opercle is prominent among the many skull bones distinguishable (Bowne 1994) in these side views of the stickleback head. The opercles of the two freshwater lacustrine fish (B, C) differ from the elongated bone of local oceanic fish (A; representing the putative ancestral morphology). All three sites were marine habitats along the shore of the island before the 3 m uplift accompanying a 1964 earthquake (Gelmond et al. 2009). Points along the edge of the opercle in A show the positions of the nine landmarks digitized for morphometric analyses, and the wire-frame diagrams to the right compare the morphologies in the manner used in following figures. In (B), we indicate the prominent dilation (double headed arrow)—diminution (single headed arrow) shape change characterizing opercle evolution between oceanic and freshwater populations globally. Scale bar: 2 mm.

Methods

DATASETS

Table 1 summarizes characteristics of the populations of threespine stickleback in our study. For the wild-captured fish, we sampled a total of 743 individuals from 22 populations (eight oceanic and 14 freshwater habitats) located in five geographical regions. Among the six sites sampled from South Central Alaska, we include three for which we previously described opercle shape using geometric morphometrics (Rabbit Slough, Mud Lake, and Visnaw Lake; Kimmel et al. 2008). Several of the populations have not been described previously, whereas some

Table 1. Populations.

Region Population	Habitat	Armor	Latitude (N)	Longitude (W)	*n*	SL Mean ±SEM	CS Mean ±SEM	PC1 Mean ±SEM	PC2 Mean ±SEM
South Central Alaska									
Rabbit Slough (RS)	o(a)	C	61.5333	−149.2500	27	71.48+1.12	8.984±0.154	0.0719±0.0044	−0.0044±0.0047
Bear Paw Lake (BP)	f(d)	l	61.6139	−149.7556	30	42.46±0.43	4.850±0.060	−0.0690±0.0048	−0.0092±0.0051
Boot Lake (BT)	f(s)	l	61.7167	−150.1167	29	44.88±0.78	5.183±0.109	−0.0624±0.0051	−0.0185±0.0048
High Ridge Lake (HR)	f(d)	m	61.5783	−149.1778	64	43.05±0.83	4.931±0.111	−0.0313±0.0032	−0.0091±0.0035
Mud Lake (MU)	f(s)	l	61.5625	−148.9486	33	47.91±1.00	5.759±0.132	−0.0263±0.0061	0.0125±0.0050
Visnaw Lake (VI)	f(d)	l	61.6194	−149.6769	44	60.99±0.55	7.758±0.087	−0.0515±0.0044	−0.0057±0.0032
Middleton Island									
Golf Ball Bay	o(m)	c	59.4604	−146.2966	30	64.46±0.66	7.838±0.104	0.0646±0.0050	0.0215±0.0043
Angry Gull Swamp (AG)	f(s)	l	59.4368	−146.3111	30	49.15±0.78	5.727±0.124	−0.0144±0.0067	0.0161±0.0050
Eagle Nest Pond (EN)	f(s)	l	59.4623	−146.2977	30	49.59±0.44	5.762±0.061	−0.0011±0.0050	0.0174±0.0059
British Columbia									
Little Campbell River (LC)	o(a)	c	50.0386	−125.2716	30	61.71±0.40	7.347±0.049	0.0612±0.0050	−0.0076±0.0032
Salmon River (SR)	o(a)	c	49.1751	−122.5944	31	63.19±0.54	7.738±0.049	0.0501±0.0043	−0.0229±0.0033
Paxton Lake (benthic, PB)	f(p)	l	49.7079	−124.5255	29	50.74±1.22	6.492±0.183	−0.0155±0.0057	0.0589±0.0051
Paxton Lake (limnetic, PL)	f(p)	l	49.7079	−124.5255	30	43.76±0.74	5.259±0.124	0.0197±0.0053	−0.0234±0.0052
Oregon									
Cushman Slough (CS)	o(a)	c	43.9868	−124.0420	28	51.39±0.42	6.162 + 0.079	0.0350±0.0051	−0.0103±0.0045
Millport Slough (MS)	o(a)	c	44.8875	−123.9973	30	58.21±0.99	7.202±0.114	0.0476±0.0042	0.0044±0.0048
South Jetty (SJ)	o(?)	c	44.0039	−124.1347	30	51.70±0.94	6.320±0.118	0.0018±0.0060	0.0067±0.0051
Lilly Lake (LI)	f(s)	l	44.0885	−124.1138	29	55.76±0.67	7.110±0.125	0.0188±0.0066	0.0009±0.0049
Pony Creek (PC)	f(s)	l	43.3704	−124.2581	52	38.43±0.77	4.842±0.110	−0.0111±0.0039	0.0007±0.0043
River Bend (RB)	f(s)	m	44.0778	−123.0268	28	42.87±0.71	5.449±0.091	−0.0376±0.0080	−0.0168±0.0066
Iceland									
Hvassahraun Bay (HV)	o(m)	m	64.0202	−22.1568	42	51.55±0.51	6.089 + 0.055	0.0585±0.0051	0.0247±0.0044
Skorraddalsvatn Lake (SK)	f(d)	l	64.5216	−21.5134	31	47.95±0.63	4.927±0.078	−0.0148±0.0053	−0.0492±0.0050
Thingvallatn Lake (TV)	f(s)	l	64.2458	−21.0542	37		3.567±0.118	−0.0353±0.0045	0.0130±0.0057
Laboratory-reared Juveniles									
RS half-sibling families		c			499	28.11±0.07	3.061±0.009	0.0469±0.0011	−0.0398±0.0011
RS single pair family		c			32	28.79±0.31	3.175±0.036	0.0226±0.0046	−0.0580±0.0027
BP single pair family		l			33	26.50±0.20	2.930±0.028	−0.0361±0.0037	−0.0595±0.0031

The names of the Middleton Island sites and the Cushman, South Jetty, and River Bend sites in Oregon are unofficial.

Habitat; f = freshwater (d = deep, p = benthic–limnetic species pair, s = shallow) o = oceanic (a = anadromous m: marine). Armor; c = complete set of lateral plates, l =low plated, m = population is mixed with respect to plate numbers.

SL = standard length (mm), SEM = Standard error of the mean, CS= Centroid size of the opercle (arbitrary units), PC1, PC2 = Opercle shape summary variables (PC scores, arbitrary units), computed excluding the three laboratory-reared juvenile populations.

information on ecology and evolution is available for Rabbit Slough, Boot, Bear Paw, Mud, and Visnaw Lakes (Bell et al. 1985, 1993; Francis et al. 1986; Walker 1997; Walker and Bell 2000; Cresko et al. 2004; Karve et al. 2008; Hohenlohe et al. 2010); the Middleton Island sites (Gelmond et al. 2009); and Paxton Lake (McPhail 1992; Schluter 1993; Taylor and McPhail 2000).

For our estimation of **G,** we used laboratory-reared half-sibling families of juveniles of Rabbit Slough ancestry. We crossed each of 50 sires to two dams (100 total), yielding 100 half-sibling families. We sampled five progeny from each family (four in one case) and grew them in a salinity of about 1 ppt to mimic the freshwater habitat. McGuigan et al. (2010a) provide details of the breeding design and stickleback husbandry. To estimate the oceanic-freshwater divergence vector for laboratory-reared juvenile fish ($\boldsymbol{d_{LJ}}$), we use single pair families of Rabbit Slough and Bear Paw Lake ancestry, rearing the fish to the same standard length as the aforementioned half-sibling families. Fry from each of these two families were reared in groups of 30 fish in 10-L aquaria at a salinity of approximately 6 ppt. Further details of our general husbandry protocols are available at: http://stickleback.uoregon.edu/index.php/. This work complied with all University of Oregon animal care requirements.

MORPHOMETRIC ANALYSES

We characterized opercle shapes through landmark-based geometric morphometrics (Zelditch et al. 2004) as described previously (Kimmel et al. 2008). Briefly, landmarks were recorded (tpsDig2, version 2.04; Rohlf 2008a) from images of left-side

views of the heads (Fig. 1) from formaldehyde-preserved fish, stained with Alizarin Red. The landmarks were Procrustes least squares superimposed in tpsRelw (version 1.46; Rohlf 2008b); four of the nine landmarks (numbers 4, 5, 6, 8; see Fig. 1A) were sliding semi-landmarks (Kimmel et al. 2008). To facilitate comparison of the direction of divergence in opercle shape with genetic lines of least resistance, Procrustes superimposed opercle landmarks of all fish in the study (wild-captured and laboratory reared, Table 1) were aligned simultaneously. Procrustes distances and visualizations of the deformations of the landmark configurations were obtained from tpsSpline (version 1.20; Rohlf 2004) and MorphoJ (version 1.02d; Klingenberg 2008). MorphoJ was also used to implement canonical variate analyses of the Procrustes-aligned residuals. Probabilities of point estimates in MorphoJ were based on permutation tests. From the Procrustes residuals of wild-caught fish, 10 nonzero principal components (PC1–10) were computed using JMP (SAS Institute Inc., Cary, NC, version 8). Note that we base our principal components analysis (PCA) only on the wild-caught fish and secondarily compute PC scores for the laboratory-reared juveniles from the PCs generated in the analysis of the wild-caught fish. Prior to analyses, PCs were mean-centered to a value of 0, implemented separately for the wild-caught data, the family data, and the laboratory-reared Rabbit Slough and Bear Paw Lake data. We use the mean-centered PCs as traits in analyses of phenotypic divergence and quantitative genetic analyses.

STATISTICAL ANALYSES OF POPULATION DIVERGENCE

The divergence in opercle shape among wild-caught fish was analyzed through multi-variate analysis of variance (MANOVA) on PC1 through PC10, where habitat (H), geographic region (R), and their interaction (HR) were fit as fixed effects, and population (P; nested within both environment and region) was fit as a random effect. The μ and ε terms are the overall mean and model error variance respectively. Analyses were conducted in SAS (SAS Institute Inc., Cary, NC, version 9.2) using PROC GLM with the model:

$$Y_{ijkl} = \mu + H_i + R_j + HR_{ij} + P_{k(ij)} + \varepsilon_{ijkl} \qquad (1)$$

To aid in interpretation of the shape changes associated with model terms, we obtained the sums of squares and cross-products (SSCP) matrices for each effect, and scaled each hypothesis SSCP matrix by the appropriate error SSCP matrix to obtain the effect matrix, which was then subjected to PCA to obtain the canonical variates associated with each effect (Table S1).

The divergences in opercle shape among wild-caught fish, $\boldsymbol{d_W}$, and among laboratory-reared juvenile fish, $\boldsymbol{d_{LJ}}$, were estimated as the first eigenvector of the variance–covariance matrix of population means (Lande 1979). The divergence vectors were normalized such that $\boldsymbol{d_W}^{\mathrm{T}}\boldsymbol{d_W} = 1$ for the estimate of wild-caught divergence, and $\boldsymbol{d_{LJ}}^{\mathrm{T}}\boldsymbol{d_{LJ}} = 1$ for the estimate of laboratory-reared juvenile divergence.

GENETIC PARAMETER ESTIMATION FROM HALF-SIBLING FAMILIES

Analyzing the mean-centered PC scores for the 499 paternal half-sibling individuals, we estimated the additive genetic (sire) covariance matrix (**G**) as four times the sire variance–covariance component matrix (Lynch and Walsh 1998), determined via mixed modeling within a restricted maximum likelihood (REML) using the MIXED procedure in SAS:

$$Y_{ijkl} = \mu + S_i + D_{j(i)} + \varepsilon_{ijkl} \qquad (2)$$

where μ is the grand mean of each trait, and sire (S) and dam (D; nested within sire) were fit as random effects. The residual variance (ε) captures random environmental (biotic and abiotic) variation among siblings sharing a tank, as well as measurement error. Statistical support for **G** was determined using factor analytic modeling (Kirkpatrick and Meyer 2004; Hine and Blows 2006). This approach tests the statistical significance of eigenvectors of **G**, providing a powerful alternative to testing the statistical support for each individual variance and covariance estimate in **G**. We implemented factor analytic modeling within the same mixed model framework in SAS as used to estimate **G** (Hine and Blows 2006; McGuigan and Blows 2010). We also used log-likelihood ratio tests to determine the statistical significance of sire variances in each individual PC trait with hierarchical models in which sire variance was estimated versus constrained to be zero. As variance components are bounded (i.e., they cannot be negative), the *P*-value for these tests is half that from the chi-squared test (Littell et al. 1996).

Results

PARALLEL OPERCLE SHAPE DIVERGENCE IS WIDESPREAD

A major objective of this study was to learn whether the pattern of opercle shape divergence that occurred when oceanic stickleback evolved in freshwater environments in South Central Alaska (Kimmel et al. 2008; Arif et al. 2009) is repeated in other more distant geographical regions. We first describe the patterns of opercle shape variation observed, then we present statistical tests of global parallel evolution. Selected skull photographs of fish from three populations sampled from one of these regions, Middleton Island in the Gulf of Alaska, illustrate the shape divergence observed across all regions in the current study (Fig. 1). The shapes of opercles of the two freshwater fish from separate lakes (Fig. 1B,C) are noticeably different from the more elongated bone

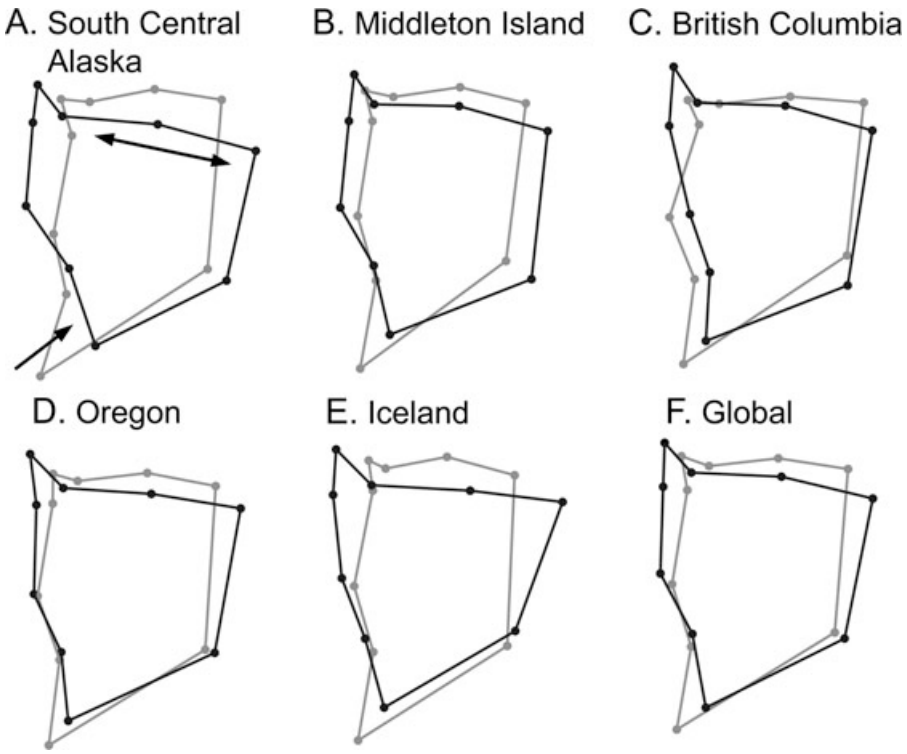

Figure 2. Opercle shape configurations reveal a common pattern of divergence between oceanic (gray) and freshwater (black) populations across regions. Figures represent total Procrustes deformations from the consensus configurations for all of the oceanic and lake populations for each region (A–E), and globally for all of the regions collectively (F). The arrows in A show the dilation–diminution shape change.

of the oceanic fish (Fig. 1A). Shown as total Procrustes deformations of landmark-based configurations of the opercle (Fig. 2), the change includes a broadening of the bone roughly along its anterior–posterior axis (double-headed arrow in Fig. 2A), which we term dilation, accompanied by a dorsal–ventral compression (single-headed arrow), or diminution. This dilation–diminution pattern is apparent for comparisons of the consensus deformation of all the freshwater populations from a given region with the reference consensus for the oceanic populations from the same geographic region (Fig. 2). Freshwater opercles vary among the different geographic regions, but this variation does not obscure the overall dilation–diminution pattern between freshwater and oceanic populations.

Both PCA and canonical variate analysis support the inference from visual inspection of the data of parallel evolution of opercle shape (Fig. 3and Fig. S1) through dimution–dilation pattern (Fig. 3 and Fig. S2). With a single exception, a putative oceanic population, South Jetty from Oregon, the average (or consensus) PC1 score for every freshwater population is lower than the consensus for every oceanic population (Table 1, Fig. 3A; see Fig. 4 for distributions of individual fish from example populations). The strong segregation of oceanic and freshwater populations along PC1 argues that habitat (oceanic vs. freshwater) is the major source of variation across the total dataset. Previous studies limited to South Central Alaska also showed this result, with PC1 capturing the same dilation–diminution variation between oceanic and freshwater opercle shapes observed in PC1 here (Kimmel et al. 2008; Arif et al. 2009). The current study extends the previous results, suggesting widespread parallel opercle bone evolution from Iceland to diverse locations along the western coast of North America.

To explicitly test this hypothesis of parallel opercle shape divergence, and to partition variance in opercle shape across habitats and regions, we used MANOVA (Table 2 and Table S1). A significant interaction between habitat and region indicates that opercle shape does not diverge identically between oceanic and freshwater habitats in all geographic regions. However, the relative magnitude of the habitat main effect F value, as compared to that for the habitat-by-region interaction, suggests that the region-specific effects of the freshwater habitat are slight relative to the general effect. Still, interpreting main effects when interactions are statistically significant should be done with caution. PC1, which explains a substantial portion of the total phenotypic variation (46%), contributed very strongly to the canonical variate of habitat divergence (Table S1, see also Table 4 below). We therefore implemented a univariate analysis of PC1 using equation 1 (see

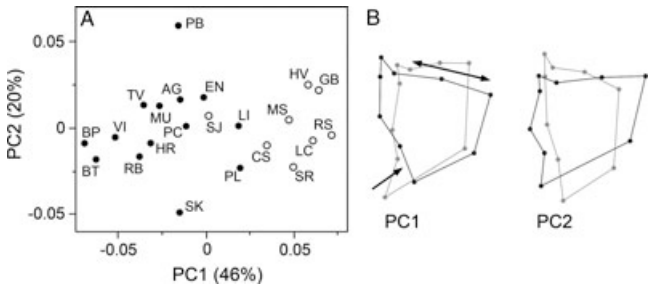

Figure 3. **(A). PC1 largely captures evolutionary divergence from oceanic to freshwater populations across disparate geographical regions. Open circles indicate consensus scores for oceanic populations, whereas filled circles indicate consensus scores for freshwater populations. Abbreviations for the populations are listed in Table 1. (B). Wire-frame diagrams showing how the opercle shape configuration changes along the PC1 and PC2 axes. The deformation from high to low PC1 (from ancestral oceanic, to descendent freshwater populations) prominently includes dilation–diminution (arrows). The deformation from high to low PC2 (from the region where the PB freshwater population maps to the region where the SK freshwater population maps) prominently includes a widening of the entire configuration.**

Table 2. **Results of MANOVA (eq 1, Methods) on wild-caught fish opercle shape.**

	Wilks' λ	*F*-Value	Degrees of freedom	*P*-value
Habitat	2.50×10^{-02}	11.68	10,3	0.034
Region	6.50×10^{-05}	3.87	40,13.23	0.005
Habitat × Region	2.07×10^{-04}	2.77	40,13.23	0.025
Population	2.12×10^{-01}	10.22	120, 5548.4	<0.001

Methods). We find that variation in PC1 is significantly associated with habitat ($F_{1,12} = 53.84$, $P < 0.001$) and with populations (nested within habitat and regions: $F_{12,722} = 15.31$, $P < 0.001$), but there is no variation among regions in how oceanic and freshwater fish differ along PC1 (habitat × regions: $F_{4,12} = 2.21$, $P = 0.129$) or among regions ($F_{4,12} = 1.04$, $P = 0.427$). Therefore, we have strong statistical evidence that opercle shape has diverged in parallel broadly across the stickleback's range, although there are also some region-specific features of the radiation, captured by PCs other than PC1 (Table S1).

OPERCLE SHAPE VARIES AMONG FRESHWATER POPULATIONS

Our primary interest in this study is the divergence in opercle shape between oceanic and freshwater habitats. However, we note that although it was of a lesser magnitude than the large ocean to freshwater divergence, there was nonetheless substantial variation among the freshwater populations in opercle shape (Table 1 and Fig. S1). Here we briefly consider two general aspects of this variation. First, the sampled populations represent radiations of different ages. In particular, freshwater habitats in South Central Alaska were colonized thousands of years ago (Hohenlohe et al. 2010), whereas the Middleton Island populations were established only 46 years ago (Gelmond et al. 2009). The freshwater populations from these two regions of Alaska differ from one another

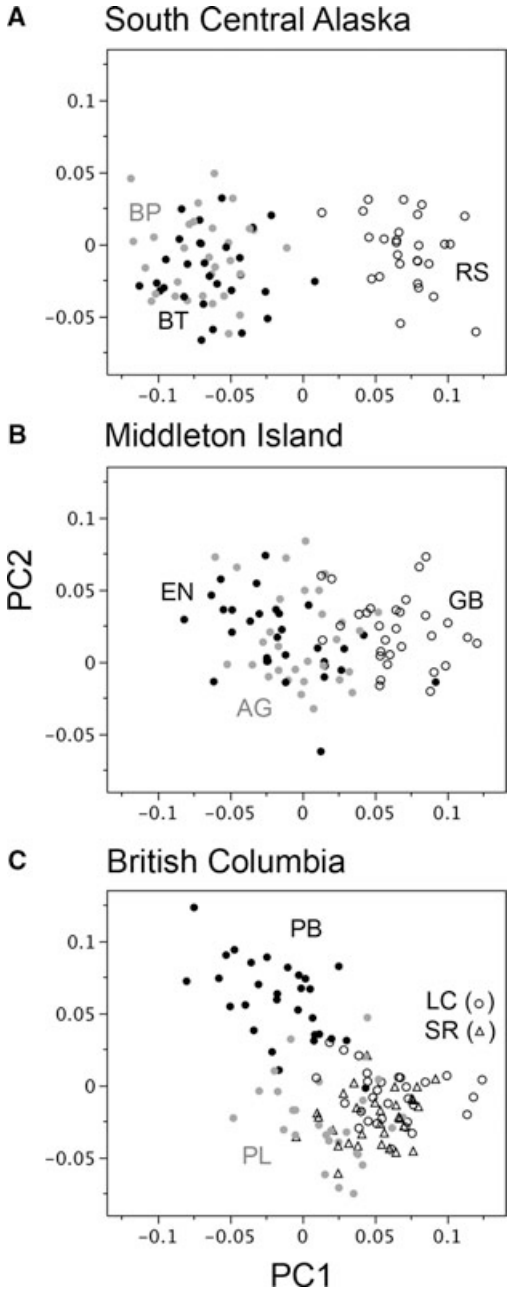

Figure 4. **Freshwater opercle shapes can show extreme (A) or milder (B) divergence along PC1 from local oceanic populations, and in some cases show marked divergence along a second axis, PC2 (C). Points represent PC scores for individual fish. Keys for the symbols are given on each panel. Abbreviations for the populations are listed in Table 1.**

in PC1 scores, with the South Central Alaskan populations lying closer to the freshwater pole of PC1 than the two Middleton Island populations (Table 1, Fig. 4A,B). Furthermore, Procrustes distances (see Zelditch et al. 2004) also suggest less oceanic to freshwater divergence for the two Middleton freshwater populations collectively (0.078), than for the five South Central Alaskan populations collectively (0.117). Hence, it is possible that the difference between oceanic and freshwater populations increases through time, but we cannot exclude other causes (see Discussion).

The second major axis of phenotypic variation in opercle shape, PC2, contributes strongly to the major axis of among population variation (Table S1). PC2, which explains 20% of the opercle shape variation across this wild-caught dataset, describes a rather uniform narrowing/widening (anterior–posterior) and lengthening/shortening (dorsal–ventral) of the opercle bone (Fig. 3B). Individuals collected from a benthic–limnetic "species-pair" from Paxton Lake (PB, British Columbia) shows opposite mean values along PC2, with benthic fish having shorter and wider opercle bones than their limnetic counterparts (Table 1 and Fig. 3A). The Paxton limnetic sticklebacks also are less divergent from local oceanic fish (Fig. 4C; Procrustes distances 0.111 and 0.059 for benthic and limnetic divergences, respectively), consistent with benthic morphology being more derived. The contrast observed here is similar to other morphological changes along the well-known benthic–limnetic axis of variation (McPhail 1992; Schluter 1993; Robinson and Wilson 1994; Cresko and Baker 1996; Taylor and McPhail 2000), which is associated with the freshwater trophic ecology of stickleback, and is likely due to intraspecific competition for benthic macroinvertebrates and planktonic prey (Bolnick 2004; Bolnick and Lau 2008). Further work is needed to determine if this PC2 axis of opercle variation is likewise due to competition for trophic resources.

EVIDENCE FOR GENETIC CONSTRAINT ON OPERCLE SHAPE DIVERGENCE

The second objective of our study was to learn whether features of the genetic architecture of the oceanic ancestor might have influenced evolution toward the dilation–diminution pattern we observe globally in the freshwater populations. Estimating **G** from a standard half-sibling breeding design with fish from Rabbit Slough, we find moderate levels of additive genetic variance in the individual opercle shape traits, with heritabilities ranging from zero (PC3) to 0.82 (PC2) (Table 3). PCs 2, 4, 5, and 9 are each associated with statistically significant genetic variance (Table 3).

To investigate genetic constraints on opercle shape evolution, we first followed Lande (1979) in describing the linear direction of phenotypic divergence as the first eigenvector of the population means. As might be expected from the association between PC1 and habitat divergence that we described above, PC1 dominates the divergence vector describing variation in population mean opercle shape in the wild ($\boldsymbol{d_W}$) and the laboratory ($\boldsymbol{d_{LJ}}$) (Table 4; vector correlation between $\boldsymbol{d_W}$ and $\boldsymbol{d_{LJ}} = 0.87$; between $\boldsymbol{cv_H}$ and $\boldsymbol{d_W} = 0.96$). The similarity of the laboratory and wild divergence vectors indicates that the dilation–diminution pattern of divergence in opercle shape is maintained in fish reared under a common garden laboratory environment, and therefore is not subject to significant phenotypic plasticity. Furthermore, the phenotypic differences are already present in relatively young fish of similar age (and size, Table 1) to the sets of half-siblings used to estimate **G** (see also Kimmel et al. 2008).

We use these quantitative genetic data to ask whether $\boldsymbol{g_{max}}$ by itself, or the entire structure of **G**, could explain the global pattern of parallel evolution. First, we determined whether the direction of divergence was associated with $\boldsymbol{g_{max}}$ or any other eigenvector of **G**. This result can be most easily visualized for the first two eigenvectors of **G** by comparing the within population pattern of genetic covariation with the direction of between population divergence (Fig. 5). However, we also tested each eigenvector to see if this could explain the pattern of global parallel divergence. The strongest correlation between the direction of divergence and any eigenvector of **G** was 0.54 (a 57.9° angle between the two vectors) and 0.46 (62.5°) for $\boldsymbol{d_W}$ and $\boldsymbol{d_{LJ}}$, respectively. For the wild-caught divergence, this maximum association was with both $\boldsymbol{g_{max}}$ and $\boldsymbol{g_3}$, whereas the laboratory divergence was most strongly associated with $\boldsymbol{g_3}$. The correlation between $\boldsymbol{d_{LJ}}$ and $\boldsymbol{g_{max}}$ was 0.39 (66.7°). Because these correlations are considerably smaller than one, we interpret them as being weak. However, we do recognize that it is difficult to interpret the evolutionary constraints described by correlations that differ from zero or one (Conner 2003; Brakefield 2006; Hansen and Houle 2008; Agrawal and Stinchcombe 2009).

We infer that the relatively low correlation between eigenvectors of **G** and the direction of divergence occurs because PC1 strongly dominates the direction of divergence, while the eigenvectors of **G** describe similar contributions from different PCs. Notably, the genetic variance in major eigenvectors of **G** is greater than in individual traits, consistent with the interpretation that more than one trait contributes to each eigenvector of **G** (Table 4). For example, although PC1 contributes strongly to $\boldsymbol{g_{max}}$ and $\boldsymbol{g_3}$, it appears to do so for both eigenvectors of **G** via covariation with other traits. This distinction is readily apparent if we constrain all the covariances between traits (off-diagonals in Table 3) to zero (Agrawal and Stinchcombe 2009). PC1, which has the third largest V_A (after PC2 and PC4), is therefore the third eigenvector of the diagonal **G**, and the correlations between this $\boldsymbol{g_{3NC}}$ and $\boldsymbol{d_W}$ and $\boldsymbol{d_{LJ}}$, respectively, are 0.99 and 0.88 (i.e., the normalized vector loading). We further note that many of the genetic correlations involving PC1 are negative; if we arbitrarily set all contributions to eigenvectors of **G** in Table 4 to be in the

Table 3. The additive genetic variance covariance matrix, G. Variances (× 10^3) on the diagonal in bold, covariances (× 10^3) below the diagonal, and correlations above the diagonal. Heritabilities were estimated from univariate analyses of traits, and significance testing of variances was implemented in univariate models.

	h^2	PC1	PC2	PC3	PC4	PC5	PC6	PC7	PC8	PC9	PC10
PC1	0.274	**0.152**[2]	−0.394	−0.880	−0.411	0.676	−1.000	−0.631	−0.728	0.148	0.616
PC2	0.429	−0.080	**0.268**[1]	−0.175	−0.158	−0.018	0.131	−0.282	0.256	−0.390	−0.153
PC3	0.000	−0.040	−0.014	**0.000**	1.000	0.350	1.000	0.919	−1.000	−0.001	1.000
PC4	0.826	−0.080	−0.040	0.064	**0.204**[1]	−0.407	0.150	0.302	−0.015	−0.108	−0.328
PC5	0.366	0.064	−0.001	0.006	−0.040	**0.052**[1]	−0.149	−0.196	0.298	−0.582	0.254
PC6	0.064	−0.080	0.005	0.031	0.009	−0.002	**0.011**	−1.000	−0.096	−0.340	−0.328
PC7	0.202	−0.038	−0.025	0.013	0.021	−0.008	−0.022	**0.023**	0.311	−0.383	0.449
PC8	0.201	−0.035	**0.015**	−0.026	−0.002	0.008	−0.001	0.005	**0.015**	0.113	−0.415
PC9	0.552	0.011	−0.040	0.003	−0.011	−0.026	−0.011	−0.011	0.005	**0.040**[1]	−0.374
PC10	0.317	0.027	−0.008	0.018	−0.016	0.007	−0.005	0.009	−0.006	−0.009	**0.012**

[1] $P < 0.05$ from log-likelihood ratio test. [2] $P = 0.0$

Table 4. The canonical variate associated with habitat (cv_H) from the MANOVA in Table 2 (also see Table S1), the divergence vectors d_W and d_{LJ} and the eigenanalysis of G. The additive genetic variance (V_A) (× 10^3) associated with each G eigenvector (i.e., the eigenvalue) is shown, along with the percentage of the total V_A explained by each eigenvector, and the contribution of each trait (PC) to each eigenvector. Only eigenvectors of G with eigenvalues greater than zero are presented.

	cv_H	d_W	d_{LJ}	g_{max}	g_2	g_3	g_4	g_5	g_6	g_7
V_A		0.132	0.068	0.336	0.300	0.101	0.068	0.045	0.035	0.013
% Total V_A		16.99%	8.75%	37.40%	33.41%	11.28%	7.55%	5.05%	3.91%	1.40%
PC1	0.962	0.995	0.875	−0.634	−0.167	0.472	−0.225	−0.085	0.025	−0.028
PC2	0.043	0.068	0.022	0.598	−0.674	0.315	−0.195	−0.033	0.084	0.135
PC3	0.128	−0.029	0.170	0.123	0.206	0.116	0.273	−0.257	0.299	0.347
PC4	0.161	0.019	0.267	0.358	0.649	0.566	−0.219	−0.024	−0.173	0.042
PC5	−0.148	−0.053	−0.058	−0.186	−0.154	0.343	0.551	−0.012	−0.407	0.393
PC6	−0.045	0.002	0.280	0.189	0.065	−0.261	0.422	−0.451	−0.069	−0.070
PC7	0.031	0.021	−0.109	0.052	0.136	−0.068	0.130	0.709	0.312	0.149
PC8	0.068	0.035	−0.061	0.080	−0.041	−0.179	−0.010	0.379	−0.583	0.298
PC9	0.021	0.014	0.186	−0.105	0.078	−0.330	−0.501	−0.265	−0.013	0.679
PC10	0.018	0.002	0.039	−0.083	−0.023	0.115	0.199	0.074	0.515	0.357

same direction (i.e., positive covariances), the minimum angle between g_{max} and d_W and d_{LJ}, respectively, are reduced to 41.7° and 38.6°.

We tested our statistical confidence in the estimated covariance of PC1 with other traits by comparing the fit of models when covariances were estimated as compared to when they were constrained to be zero. We focused this on the covariance between PC1 and PCs 2, 4, 5, and 9. These PCs are the ones associated with the greatest V_A (Table 3), and contribute most strongly to major eigenvectors of **G**. Therefore it is the covariance between these traits and PC1 that is most likely to underlie the deviation in directions of divergence and eigenvectors of **G**. Constraining PC1 to not covary with these other traits worsened model fit (Akaike's information criterion, AIC; –38,724.1 for estimated covariances vs. –38,719.8 when covariances were held to zero). However, the log-likelihood ratio test was not significant ($\chi^2 = 3.736$, df = 4, $P = 0.443$).

Another approach to determining confidence in the estimated covariation of PC1 with other traits, and therefore our confidence in the interpretation that divergence was not strictly along eigenvectors of **G**, is factor analytic modeling with specific variance structure to test the hypothesis that PC1 shares genetic variance with other traits versus has an independent genetic basis (McGuigan and Blows 2010). Using model 2 (see Methods), we fit covariance structures at the sire level that estimated both trait-specific variances and common variances (McGuigan and Blows 2010). A model with a single common factor and specific variances best fit the data (AIC: one-factor model –30,241.8; two factor model –30,236.1). This model explained 78% of the total additive genetic variance. The estimate of trait-specific variance

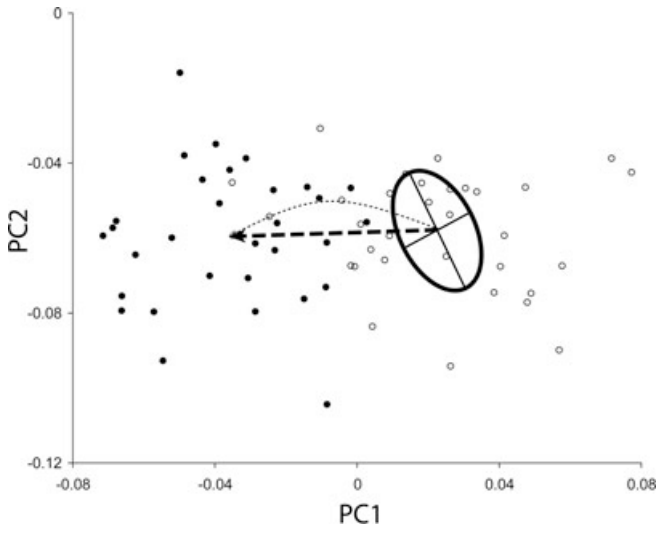

Figure 5. Leading eigenvectors of G are not aligned with the vector of evolutionary divergence. Laboratory-reared individuals from Boot Lake (filled circles) and Rabbit Slough (open circles) plotted in the previously described PC1 and PC2 phenotypic space. These individuals are from single-pair families (crosses within Boot Lake and Rabbit Slough lines), and grown to the same body size as the half-sibling families of stickleback used for the G matrix analysis. The first two axes of the G matrix (i.e., g_{max} and g_2; estimated from the Rabbit Slough half-sibling families, not shown in this figure) are superimposed (bold oval) on these points and centered on the mean of the laboratory reared single pair family of Rabbit Slough stickleback. The dashed arrow shows the vector of divergence in this space from the mean of Rabbit Slough two-dimensional G to the mean of the Boot Lake family. The dotted line shows the perturbation in the evolutionary trajectory of the population predicted by the influence of G, with the trajectory calculated under the assumption of Gaussian selection operating independently on the two traits and an intensity of selection strong enough to generate the necessary response within 1,000 to 10,000 generations.

for PC1 was zero. The single common eigenvector was similar to the g_{max} estimated from the unconstrained model (Table 4), with a vector correlation of 0.79. This common variance g_{maxC} was not closely related to d_W or d_{LJ} (52.4° and 60.0° respectively). This result suggests that PC1 is genetically constrained to covary with other traits, and supports the observation that divergence in opercle shape has not occurred along major eigenvectors of **G**.

A second perspective that we consider here on potential constraints imposed by **G** is whether the evolution of opercle shape was biased by the lack of genetic variation in particular directions of multivariate phenotypic space. Factor analytic tests of the rank of **G** indicate weak statistical support for two dimensions of **G** (two to one dimensions: $\chi^2 = 15.706$, df $= 9$, $P = 0.073$; zero to one dimension: $\chi^2 = 24.934$, df $= 10$, $P = 0.005$). The first two eigenvectors of **G**, g_{max} and g_2, are each associated with similar, relatively large amounts of additive genetic variance (Table 4), accounting for 37% and 33% of the additive genetic variance respectively. The first seven eigenvectors of **G** captured all of the genetic variance, further supporting the presence of opercle shapes for which there is no genetic variation. These genetically depauperate regions of multivariate phenotypic space can be thought of as imposing a global, absolute genetic constraint on opercle shape variation. Further support for this point comes from the effective dimensionality (Kirkpatrick 2009), which is the sum of the eigenvalues divided by the largest eigenvalue, which for our **G** is $n_D = 2.31$. This value is slightly higher than observed in other studies (Kirkpatrick 2009; Simonsen and Stinchcombe 2010), but consistent with our observation that the first two eigenvectors of **G** capture relatively similar amounts of genetic variation. Therefore, our data suggest that there are relatively few axes of phenotypic space that are evolutionarily accessible to our Rabbit Slough population of stickleback.

Despite the presence of potential absolute constraints, we find that these regions of low genetic variation in the opercle genetic architecture are unimportant for the actual trajectories of parallel opercle evolution. To do so we considered the relationship between the direction of divergence and the evolutionary accessibility of phenotypic space by directly estimating the genetic variance in the direction of divergence. We applied the normalized divergence vectors d_W and d_{LJ} to the individual half-sibling PC scores to generate univariate divergence traits, which we then subjected to genetic analysis. The genetic variance associated with d_W is 1.32×10^{-04}, and for d_{LJ} 6.80×10^{-05}, which are, respectively 39.38% and 20.23% of the maximum genetic variance associated with any linear combination of traits (i.e., of the V_A of g_{max}; Table 4). For the direction of opercle shape divergence estimated from laboratory reared juveniles, the additive genetic variance in the direction of divergence was slightly less than the mean (88% of the mean) but larger than all but the first four eigenvalues of **G** (Table 4). For the direction of divergence measured on wild-caught fish, there was above average additive genetic variance in the direction that opercle shape divergence occurred, with greater evolvability in this direction than in all but the first two eigenvectors of **G** (Table 4). As with the lack of statistical support for more than two dimensions of **G** (factor analytic results above) or in PC1 itself (Table 3), we could not statistically demonstrate that the genetic variance in the direction of divergence was greater than zero (log-likelihood ratio test of univariate divergence scores: d_W: $\chi^2 = 1.379$, $P = 0.120$, $h^2 = 0.237$; d_{LJ}: $\chi^2 = 0.610$, $P = 0.217$, $h^2 = 0.147$). Therefore, in combination with our findings of widespread parallel evolution, our results show that opercle shape divergence occurred independently and repeatedly in a direction of phenotypic space that was associated with relatively high levels of additive genetic variation. We argue below that the data are consistent with a permissive, likely not biasing, role of **G**.

Discussion

Understanding the relative contributions of similar selection regimes and genetic bias to patterns of parallel phenotypic evolution is a long-standing issue in evolutionary biology. Over relatively short time periods, the phenotypic response to directional selection may not occur strictly in the direction of greatest "increase" in fitness (i.e., not along the selection gradient), but rather may be biased toward the direction of greatest genetic variance (i.e., along $\boldsymbol{g}_{max}$, Lande 1979; Schluter 1996; Hansen and Houle 2008). In addition, the overall structure of **G** may affect the trajectory of evolving populations, even when evolution does not occur strictly along $\boldsymbol{g}_{max}$. Despite these robust theoretical predictions, the precise nature, temporal persistence, and prevalence of genetic bias during evolution in natural populations are still unclear. Here, we address the question of genetic bias by taking advantage of the global pattern of replicated and recent phenotypic evolution of freshwater populations of stickleback from oceanic ancestors. We extend our previous observation of parallel freshwater evolution of opercle shape, demonstrating that the dilation–dimution evolution of opercle shape in freshwater is a global pattern. We explicitly test whether the major axis of phenotypic variation between oceanic and freshwater populations is associated with axes of genetic variance of the putative ancestral oceanic population, and find no convincing evidence that opercle shape evolution was biased to occur along $\boldsymbol{g}_{max}$, or constrained to occur along other eigenvectors of **G**. Although the eigenvectors were not implicated in the parallel evolution, we note that the few dimensions of opercle phenotypic space are associated with additive genetic variation, and that opercle divergence occurred in a direction with above average evolvability.

OPERCLE SHAPE EVOLVES IN PARALLEL ON A GLOBAL SCALE

Extending previous studies showing the dilation–diminution pattern of opercle shape divergence within a fairly small geographic area of Alaska (Kimmel et al. 2005; Kimmel et al. 2008; Arif et al. 2009), we observe parallel evolution of opercle shape in multiple populations spread across a large swath of coastal western North America—Alaska, British Columbia, and Oregon—as well as from Iceland. The threespine stickleback lineage might have originally evolved in the Pacific basin, and subsequently spread into the Atlantic basin at least 90,000–260,000 years ago (Orti et al. 1994; Mäkinen and Merilä 2008) and possibly earlier, making the evolutionary similarities we find between Icelandic and western North American populations even more striking. Other phenotypic traits are known to have diverged in parallel in independently evolving freshwater stickleback populations, including behavior, body shape, trophic morphology, and skeletal armor (Colosimo et al. 2004, 2005; Cresko et al. 2004, 2007; Shapiro et al. 2004). Although armor and opercle shape evolution both captured variation caused by bone development, it is interesting to note that whereas parallel changes that have been described in armor involve its loss in fresh water, the changes we describe in opercles relate to continuous variation in the shape of the bone.

Our data also provide evidence that opercle evolution can be quite rapid. Middleton Island freshwater populations were divergent from the local marine ancestor despite these freshwater habitats only being created in 1964. Arif et al. (2009) report similar findings of rapid evolution of opercle shape for Loberg Lake in South Central Alaska. The rapidity of the evolution might indicate strong directional selection, but relatively little is known about the demography of the colonization. Comparing the data from Middleton Island and South Central Alaska suggests that variation in the amount of change along the axis describing divergence between oceanic and freshwater habitats (i.e., $\boldsymbol{d}_{W}$ or PC1) corresponds to the time since colonization. However, an alternative explanation for the disparity could be differences in selection in the freshwater populations from the two regions. Ongoing sampling of the Middleton Island populations to test for increasing divergence could resolve this question.

The observation that benthic and limnetic stickleback in Paxton Lake, British Columbia, have opposing values along PC2 suggests the possibility of multiple selective optima for opercle shape among different freshwater habitats. The Paxton Lake fish provide a well-known example of a benthic–limnetic species pair, in which the availability of different habitats within the lake has led to divergent evolution of fish into two trophic morphotypes, exploiting food resources on the lake bottom (macroinvertebrates) and water column (plankton), respectively (McPhail 1992; Schluter 1993; Taylor and McPhail 2000). The strong divergence of Paxton Lake benthic and limnetic populations on PC2 suggests this axis of opercle shape variation might be related to foraging ecology. In this light we note that in their study of populations in South Central Alaska (Arif et al. 2009) also attributed opercle change along the second major axis of phenotypic variation to differences in foraging ecology. The interpretation of Arif et'al. (2009) is consistent with data from the same region that whole body morphology (Walker 1997) and skull morphology (Caldecutt and Adams 1998; Willacker et al. 2010) vary along the benthic–limnetic axis. In Paxton Lake, as for other features of the benthic–limnetic species pair (Lavin and McPhail 1986, 1987; McPhail 1992), benthic opercles are more highly derived than those of the limnetic fish, which are only moderately different from the oceanic form. Deciding whether competition and/or foraging ecologies are critical factors determining opercle shape change between benthic and limnetic fish will need to be tested with more extensive sampling across allopatric benthic and limnetic freshwater populations, particularly including other lakes with sympatric species pairs in British Columbia.

DIVERGENCE IN OPERCLE SHAPE IS NOT STRONGLY BIASED BY MAJOR AXES OF MULTIVARIATE GENETIC VARIATION

We used sticklebacks derived from Rabbit Slough, a population that likely represents the ancestor of the derived freshwater populations in South Central Alaska (Walker and Bell 2000; Aguirre et al. 2008; Hohenlohe et al. 2010), to estimate the genetic variance–covariance matrix (**G**) of opercle shape. We therefore were able to provide a meaningful test of the hypothesis that the evolution of opercle shape in novel freshwater habitats was biased by the genetic architecture of oceanic stickleback that initially invaded these habitats. We first asked whether the major axis of genetic variation determined the pattern of divergence among populations. We find little evidence that opercle shape divergence was strongly biased along $\boldsymbol{g}_{max}$, or any other eigenvectors of **G**. This result contrasts with Schluter's (1996) findings. The angle between our divergence and **G**-vector estimates were large (60–67°) relative to that reported by Schluter (1996) (18°) for foraging traits in threespine stickleback. Furthermore, the direction of divergence was associated to a similar extent with two (orthogonal) vectors of **G**, $\boldsymbol{g}_{max}$ and $\boldsymbol{g}_3$. Recently, Berner et al. (2010) considered the same foraging traits as in Schluter's study, but in geographically distinct populations, and found 32–55° between the major axis of phenotypic variation within a marine population and phenotypic divergence between this population and derived freshwater stickleback. Whether stronger or weaker associations should be expected for studies of genetic or phenotypic variances and covariances is not clear. Chenoweth et al. (2010) suggested that whether phenotypic divergence occurs along $\boldsymbol{g}_{max}$ will be determined by two factors. First, $\boldsymbol{g}_{max}$ will exhibit the strongest association with divergence when it accounts for much of the genetic variation (**G** is "ill-conditioned"). Although our **G** is singular (i.e., has negative eigenvalues; see below), $\boldsymbol{g}_{max}$ and $\boldsymbol{g}_2$ capture similar portions of genetic variance, suggesting bias along $\boldsymbol{g}_{max}$ should not be expected for opercle shape.

Second, $\boldsymbol{g}_{max}$ will bias evolution to a greater extent when selection is in a direction associated with very little genetic variation. We have not yet measured the selection acting on opercle bone shape in either oceanic or freshwater populations. Selection in directions associated with very little genetic variation has been reported for sexually selected traits, which are under persistent directional selection or stabilizing selection (Hine et al. 2004; Hunt et al. 2007; Chenoweth et al. 2010; see also Simonsen and Stinchcombe 2010). In the current study, we have no reason to expect an absence of genetic variation in the direction of selection. Even if persistent stabilizing selection acted on opercle shape in the oceanic ancestor and depleted genetic variation, the colonization of freshwater habitat most likely involves a shift in the adaptive optimum, and thus a change in the direction of selection. This change would then alleviate any constraint caused by a lack of genetic variation in the direction of selection, and therefore reducing the bias imposed by $\boldsymbol{g}_{max}$.

A caveat to our interpretation that genetic bias is weak or lacking is that the modest association we observe between $\boldsymbol{g}_{max}$ and $\boldsymbol{d}$ might reflect the dissipation of a once stronger genetic bias over extensive periods of evolutionary divergence (for discussion see Schluter 1996). The Bear Paw Lake population that we used to determine the divergence vector $\boldsymbol{d}_{LJ}$ has likely been isolated from its oceanic ancestor for many thousands of years, which might be long enough for such dissipation to occur. However, as we have noted, the direction of phenotypic divergence between oceanic and freshwater populations appears to be markedly consistent across freshwater stickleback populations of different ages, including the 46-year-old Middleton Island populations, therefore suggesting that the direction of the divergence vector might not change markedly over thousands of generations. Furthermore, the age of some populations within our analysis is comparable to that of stickleback comparisons in Schluter (1996), who reported a relatively close association between the direction of divergence and $\boldsymbol{g}_{max}$ for foraging traits in threespine stickleback.

THE OVERALL STRUCTURE OF G HAS NOT BIASED OPERCLE EVOLUTION

Comparing divergence in opercle shape with the major axes of genetic variation in oceanic stickleback captures one aspect of evolutionary bias caused by the genetic architecture of traits. However, even without a clear association between major genetic axes and divergence, the overall multivariate structure of genetic variation and covariation could affect the evolutionary trajectory of a population, causing it to differ from that expected simply due to the fitness landscape. For example, an absolute constraint—an absence of any evolutionary response despite strong selection—could occur if some regions of phenotypic space are difficult to reach by evolving populations because of a lack of genetic variation. Similarly, although divergence may not occur in precise accord with a major axis of variation, it can still be biased in a direction that is associated with more genetic variation in the putative ancestor. Demonstrating absolute genetic constraints caused by a complete absence of genetic variance is difficult (Mezey and Houle 2005; Kirkpatrick 2009). Nonetheless, the majority of genetic variance in opercle shape was concentrated in relatively few dimensions, suggesting that some regions of the opercle bone morphospace are likely to be evolutionarily inaccessible. These regions of phenotypic space that are depauperate for genetic variation create a potential for genetic bias in stickleback opercle evolution. Similar biases in the distribution of genetic variation have been observed for other traits in other taxa (Hine and Blows 2006; Kirkpatrick 2009; Simonsen and Stinchcombe 2010).

Our results show that these regions of potential absolute constraint due to lack of genetic variation unimportant for the actual

parallel opercle evolution. Although we were unable to provide statistical support for genetic variance in the direction of oceanic-freshwater divergence, we note that the estimated genetic variance for this trait combination was greater than for the third (laboratory divergence) or fourth (wild divergence) eigenvector of **G**; that is, evolution may well have occurred in a direction associated with greater genetic variation than most directions of morphospace. A similar result has been reported for the divergence of wing shape in *Drosophila*, which also occurred in directions with greater than average evolvability (Hansen and Houle 2008), and in the stickleback study reported by Berner et al. (2010) in which trophic morphology divergence occurred in a direction of morphospace associated with relatively high levels of phenotypic variation within a putatively ancestral population (see Hansen and Voje 2011).

In the absence of a fitness landscape, we cannot completely rule out the possibility that the pattern of genetic covariation among traits has to some extent constrained opercle evolution within these populations. This is particularly true given the presence of regions of morphospace with little genetic variation and the slightly greater than average evolvability in the direction of divergence. A key strength of our study is that the global pattern of parallel evolution argues against this view. We do not observe opercle evolution occurring in each geographic region in one of many alternative directions of phenotypic space. Instead, we see opercles evolve to the very same regions of morphospace across the globe, despite the fact that other acceptable regions of phenotypic space appear to exist. Thus, even though there is some potential for **G** to perturb evolutionary trajectories in this system, a consistent pattern of parallel evolution suggests that this is not the case (see Zeng 1988). For example, if we assume that the direction of divergence in fact does represent the history of natural selection, then the trajectory of evolution from the oceanic to freshwater phenotype is only slightly deflected by **G** from the most direct approach to the freshwater fitness optimum (Fig. 5). Both the parallel evolution and the absence of a strong effect of **G** on the trajectory therefore point toward natural selection, and not genetic bias, as the main reason for the evolution of opercle bone shape in freshwater habitats.

CONCLUSION

A primary goal of evolutionary biology is to understand the relative importance of population processes contributing to the origin, maintenance, and sorting of genetic and phenotypic variation. Patterns of parallel or convergent evolution of phenotypes could be due to some combination of natural selection and the channeling or biasing effects of genetic architectures. There have been few direct experimental tests of genetic bias in the parallel evolution of phenotypes. We have extended our earlier work to demonstrate that parallel opercle shape divergence between oceanic and lake populations of stickleback occurs in geographically disparate regions, arguing either for the presence of globally similar selection regimes or the presence of strongly and consistently biasing genetic architecture in the ancestral oceanic populations. In contrast to the predictions for a strong role of biasing genetic architecture, we detected no strong association between the direction of divergence and specific eigenvectors describing the structure of additive genetic variation–covariation in the oceanic populations. We did observe that additive genetic variation was very small in many directions of phenotypic space, and that opercle shape divergence occurred repeatedly in a direction associated with a larger than average amount of genetic variance. The parallel nature of opercle shape divergence on a global scale supports the inference that, although the divergence occurred in a subset of the phenotypic space associated with significant genetic variation, the specific direction in which divergence occurred most strongly reflects the direction of divergent selection, and not the strong biasing effects of genetic architecture. Taken together, these results contribute to a more nuanced view of how selection and genetic architecture of traits can interact to produce phenotypic evolution. However, significant work remains to be completed in this system. Future experiments will need to characterize the adaptive landscape, to identify the genes contributing to the evolving traits, and to determine the effects of these loci on the genetic architecture of the traits. Stickleback are amenable to these various approaches, and a more complete understanding will certainly emerge in coming years. By performing similar research in many organismal systems, general themes about the relative importance of selection, and internal constraint in parallel phenotypic evolution are likely to emerge.

ACKNOWLEDGMENTS

This research was funded by the US National Science Foundation grants (IOS-0618738 and IOS-0642264) and the University of Oregon startup funds (W.A.C.). KM is supported by The University of Queensland and the Australian Research Council. D. Schluter supplied the fish from British Columbia. R. Bernhardt, B. Furin, H. Weigner, C. O'Brien, and C. Hulslander helped with fish collection and husbandry. P. Morrow assisted with preparation of the manuscript. We thank T. Hansen and J. Kelly for helpful comments on the manuscript, and J. Kelly for suggesting the evolutionary trajectory approach used in Fig. 5.

LITERATURE CITED

Agrawal, A. F., and J. R. Stinchcombe. 2009. How much do genetic covariances alter the rate of adaptation? Proc. Biol. Sci. 276: 1183–1191.

Aguirre, W. E., K. E. Ellis, M. Kusenda, and M. A. Bell. 2008. Phenotypic variation and sexual dimorphism in anadromous threespine stickleback: implications for postglacial adaptive radiation. Biol. J. Linn. Soc. 95:465–478.

Arif, S., W. E. Aguirre, and M. A. Bell. 2009. Evolutionary diversification of opercle shape in Cook Inlet threespine stickleback. Biol. J. Linn. Soc. 97:832–844.

Arnold, S. J. 1992. Constraints on phenotypic evolution. Am. Nat. 140: S85–S107.

Badyaev, A. V., and G. E. Hill. 2000. The evolution of sexual dimorphism in the house finch. I. Population divergence in morphological covariance structure. Evolution 54:1784–1794.

Begin, M., and D. A. Roff. 2003. The constancy of the G matrix through species divergence and the effects of quantitative genetic constraints on phenotypic evolution: a case study in crickets. Evolution 57: 1107–1120.

———. 2004. From micro- to macroevolution through quantitative genetic variation: positive evidence from field crickets. Evolution 58: 2287–2304.

Beldade, P., K. Koops, and P. Brakefield. 2002. Developmental constraints versus flexibility in morphological evolution. Nature 416:844–847.

Bell, M. A., and S. A. Foster, eds. 1994. The evolutionary biology of the threespine stickleback. Oxford Univ. Press, Oxford; New York.

Bell, M. A., R. C. Francis, and A. C. Havens. 1985. Pelvic reduction and its directional asymmetry in threespine sticklebacks from the Cook Inlet Region, Alaska. Copeia 1985:437–444.

Bell, M. A., G. Orti, J. A. Walker, and J. P. Koenings. 1993. Evolution of pelvic reduction in threespine stickleback fish: a test of competing hypotheses. Evolution 47:906–914.

Berner, D., M. Roesti, A. P. Hendry, and W. Salzburger. 2010. Constraints on speciation suggested by comparing lake-stream stickleback divergence across two continents. Mol. Ecol. 19:4963–4978.

Blows, M. W., and M. Higgie. 2003. Genetic constraints on the evolution of mate recognition under natural selection. Am. Nat. 161:240–253.

Bolnick, D. I. 2004. Can intraspecific competition drive disruptive selection? An experimental test in natural populations of sticklebacks. Evolution 58:608–618.

Bolnick, D., and O. L. Lau. 2008. Predictable patterns of disruptive selection in three-spine stickleback. Am. Nat. 172:1–11.

Bowne, P. S. 1994. Systematics and morphology of the Gasterosteiformes. Pp. 28–60 *in*: A. M. Bell and S. A. Foster, (eds.), The evolutionary biology of the threespine stickleback. Oxford Univ. Press, Oxford; New York.

Brakefield, P. M. 2006. Evo-devo and constraints on selection. Trends Ecol. Evol. 21:362–368.

Caldecutt, W. J., and D. C. Adams. 1998. Morphometrics of trophic osteology in four ecotypes of the threespine stickleback, *Gasterosteus aculeatus*. *Copeia* 1998:827–838.

Chenoweth, S.F., H.D. Rundle, and M.W. Blows. 2010. Experimental evidence for the evolution of indirect genetic effects: changes in the interaction effect coefficient, *psi*, due to sexual selection. Evolution 64:1849–1856.

Cheverud, J. 1984. Quantitative genetics and developmental constraints on evolution by selection. J. Theor. Biol. 110:155–171.

Colosimo, P. F., C. L. Peichel, K. S. Nereng, B. K. Blackman, M. D. Shapiro, D. Schluter, and D. M. Kingsley. 2004. The genetic architecture of parallel armor plate reduction in threespine sticklebacks. PLoS Biol. 2:635–641.

Colosimo, P. F., K. E. Hosemann, S. Balabhadra, G. Villareal, M. Dickson, J. Grimwood, J. Schmutz, R. Myers, D. Schluter, and D. M. Kingsley (2005). Widespread parallel evolution in sticklebacks by repeated fixation of ectodysplasin alleles. Science 307:1928–1933.

Conner, J. K. 2003. Artificial selection: a powerful tool for ecologists. Ecology 84:1650–1660.

Cresko, W. A., and J. A. Baker. 1996. Two morphotypes of lacustrine threespine stickleback, *Gasterosteus aculeatus*, in Benka Lake, Alaska. Environ. Biol. Fish. 45:343–350.

Cresko, W.A., K. McGuigan, P.C. Phillips, and J. H. Postlethwait. 2007. Developmental genetic basis of microevolution in threespine stickleback: progress and promise. Genetica 129:105–126.

Cresko, W. A., A. Amores, C. Wilson, J. Murphy, M. Currey, P. C. Phillips, M. A. Bell, C. B. Kimmel, and J. H. Postlethwait. 2004. Parallel genetic basis for repeated evolution of armor loss in Alaskan threespine stickleback populations. Proc. Natl. Acad. Sci. USA 101:6050–6055.

Dickerson, G. E. 1955. Genetic slippage in response to selection for multiple objectives. Cold Spring Harb. Sym. 20:213–224.

Endler, J. A. 1986. Natural selection in the wild. (MPB-21). Princeton Univ. Press, Princeton, NJ.

Francis, R. C., J. V. Baumgartner, A. C. Havens, and M. A. Bell. 1986. Historical and ecological sources of variation among lake populations of threespine sticklebacks, *Gasterosteus aculeatus,* near Cook inlet, Alaska Can. J. Zool. 64:2257–2265.

Gelmond, O., F. A. von Hippel, and M. S. Christy. 2009. Rapid ecological speciation in three-spined stickleback *Gasterosteus aculeatus* from Middleton Island, Alaska: the roles of selection and geographic isolation. J. Fish. Biol. 75:2037–2051.

Hansen, T., and D. Houle. 2008. Measuring and comparing evolvability and constraint in multivariate characters. J. Evol. Biol. 21:1201–1219.

Hansen, T. F., and K. L. Voje. 2011. Deviation from the line of least resistance does not exclude genetic constraints: a comment on Berner et al. (2010). Evolution 65:1821–1822.

Hendry, A. P., E. B. Taylor, and J. D. McPhail. 2002. Adaptive divergence and the balance between selection and gene flow: lake and stream stickleback in the Misty system. Evolution 56:1199–1216.

Hine, E., and M. Blows. 2006. Determining the effective dimensionality of the genetic variance–covariance matrix. Genetics 173:1135–1144.

Hine, E., S. F. Chenoweth, and M. W. Blows. 2004. Multivariate quantitative genetics and the Lek paradox: genetic variance in male sexually selected traits of *Drosophila serrata* under field conditions. Evolution 58:2754–2762.

Hohenlohe, P. A., S. Bassham, P. D. Etter, N. Stiffler, E. A. Johnson, and W. A. Cresko. 2010. Population genomics of parallel adaptation in threespine stickleback using sequenced RAD tags. PLoS Genet. 6:e1000862.

Hunt, J., J. B. Wolf, and A. J. Moore. 2007. The biology of multivariate evolution. J. Evol. Biol. 20:1–8; discussion 39–44.

Jones, A. G., S. J. Arnold, and R. Bürger. 2003. Stability of the G-matrix in a population experiencing pleiotropic mutation, stabilizing selection, and genetic drift. Evolution 57:1747–1760.

Karve, A. D., F. A. von Hippel, and M. A. Bell. 2008. Isolation between sympatric anadromous and resident threespine stickleback species in Mud Lake, Alaska. Environ. Biol. Fish 81:287–296.

Kimmel, C., B. Ullmann, C. Walker, C. Wilson, M. Currey, P. Phillips, M. Bell, J. Postlethwait, and W. A. Cresko. 2005. Evolution and development of facial bone morphology in threespine sticklebacks. Proc. Natl Acad. Sci. USA 102:5791–5796.

Kimmel, C. B., W. E. Aguirre, B. Ullmann, M. Currey, and W. A. Cresko. 2008. Allometric change accompanies opercular shape evolution in Alaskan threespine sticklebacks. Behaviour 145:669–691.

Kimmel, C. B., A. DeLaurier, B. Ullmann, J. Dowd, and M. McFadden. 2010. Modes of developmental outgrowth and shaping of a craniofacial bone in zebrafish. PLoS One 5:e9475.

Kirkpatrick, M. 2009. Patterns of quantitative genetic variation in multiple dimensions. Genetica 136:271–284.

Kirkpatrick, M., and K. Meyer. 2004. Direct estimation of genetic principal components: simplified analysis of complex phenotypes. Genetics 168:2295–2306.

Klingenberg, C. P. 2008. Novelty and "homology-free" morphometrics: what's in a name? Evol. Biol. 35:186–190.

Lande, R. 1979. Quantitative genetic analysis of multivariate evolution, applied to brain: body size allometry. Evolution 33:402–416.

Lande, R., and S. J. Arnold. 1983. The measurement of selection on correlated characters. Evolution 37:1210–1126.

Lavin, P. A., and J. D. McPhail. 1986. Adaptive divergence of trophic phenotype among freshwater populations of the threespine stickleback (*Gasterosteus aculeatus*). Can. J. Fish. Aquat. Sci. 43:2455–2463.

———. 1987. Morphological divergence and the organization of trophic characters among lacustrine populations of the threespine stickleback (*Gasterosteus aculeatus*). Can. J. Fish. Aquat. Sci. 44:1820–1829.

Littell, R., G. A. Milliken, W. W. Stroup, and R. D. Wolfinger. 1996. SAS system for mixed models. SAS Institute, Inc.

Lynch, M., and B. Walsh. 1998. Genetics and analysis of quantitative traits. Sinauer Associates Inc., Sunderland, MA.

Mäkinen, H. S., and J. Merilä. 2008. Mitochondrial DNA phylogeography of the three-spined stickleback (*Gasterosteus aculeatus*) in Europe—evidence for multiple glacial refugia. Mol. Phylogenet. Evol. 46: 167–182.

McGuigan, K., and M. W. Blows. 2007. The phenotypic and genetic covariance structure of drosphilid wings. Evolution 61:902–911.

———-. 2010. Evolvability of individual traits in a multivariate context: partitioning the additive genetic variance into common and specific components. Evolution 64:1899–1911.

McGuigan, K., S. F. Chenoweth, and M. W. Blows. 2005. Phenotypic divergence along lines of genetic variance. Am. Nat. 165:32–43.

McGuigan, K., N. Nishimura, M. Currey, D. Hurwit, and W. A. Cresko. 2010a. Quantitative genetic variation in static allometry in the threespine stickleback. Soc. Integr. Comp. Biol. 50:1067–1080.

McGuigan, K., L. Rowe, and M. W. Blows. 2010b. Pleiotropy, apparent stabilizing selection and uncovering fitness optima. Trends Ecol. Evol. 26:22–29.

McKinnon, J. S., S. Mori, B. K. Blackman, L. David, D. M. Kingsley, L. Jamieson, J. Chou, and D. Schluter. 2004. Evidence for ecology's role in speciation. Nature 429:294–298.

McPhail, J. D. 1992. Ecology and evolution of sympatric sticklebacks (Gasterosteus): evidence for a species-pair in Paxton Lake, Texada Island, British Columbia. Can. J. Zool. 70:361–369.

Merilä, J., and M. Björklund. 1999. Population divergence and morphometric integration in the greenfinch (*Carduelis chloris*)—evolution against the trajectory of least resistance? J. Evol. Biol. 12:103–112.

Mezey, J. G., and D. Houle. 2005. The dimensionality of genetic variation for wing shape in *Drosophila melanogaster*. Evolution 59:1027–1038.

Miller, C. T., S. Beleza, A. A. Pollen, D. Schluter, R. A. Kittles, M. D. Shriver, and D. M. Kingsley. 2007. cis-Regulatory changes in Kit ligand expression and parallel evolution of pigmentation in sticklebacks and humans. Cell 131:1179–1189.

Orti, G., M. A. Bell, T. E. Reimchen, and A. Meyer. 1994. Global survey of Mitochondrial-DNA sequences in the threespine stickleback—evidence for recent migrations. Evolution 48:608–622.

Price, T., M. Turelli, and M. Slatkin. 1993. Peak shifts produced by correlated response to selection. Evolution 47:280–290.

Robinson, B., and D. S. Wilson. 1994. Character release and displacement in fishes: a neglected literature. Am. Nat. 144:596–627.

Rohlf, F. 2008a. tpsDig2, digitize landmarks and outlines, version 2.12. Department of Ecology and Evolution, State Univ. of New York at Stony Brook.

———. 2008b. tpsRelw, relative warps analysis, version 1.46. Department of Ecology and Evolution, State Univ. of New York at Stony Brook.

———. 2004. tpsSpline, thin-plate spline, version 1.20. Department of Ecology and Evolution, State Univ. of New York at Stony Brook.

Schluter, D. 1993. Adaptive radiation in sticklebacks: size, shape and habitat use efficiency. Ecology 74:699–709.

———. 1996. Adaptive radiation along genetic lines of least resistance. Evolution 50:1766–1774.

———. 2000. The ecology of adaptive radiation. Oxford Univ. Press, Oxford.

Simonsen, A. K., and J. R. Stinchcombe. 2010. Quantifying evolutionary genetic constraints in the Ivyleaf morning glory, *Ipomoea hederacea*. Int. J. Plant Sci. 171:972–986.

Stebbins, G. L. 1974. Flowering plants: evolution above the species level. Belknap Press, Cambridge, MA.

Steppan, S. J., P. C. Phillips, and D. Houle. 2002. Comparative quantitative genetics: evolution of the G matrix. Trends Ecol. Evol. 17:320–327.

Taylor, E. B., and J. D. McPhail. 2000. Historical contingency and ecological determinism interact to prime speciation in sticklebacks, Gasterosteus. Proc. R. Soc. Lond. B. 267:2375–2384.

Taylor E.B., J.D. McPhail, D. Schluter. 1997. History of ecological selection in sticklebacks: uniting experimental and phylogenetic approaches. Pp. 511–534 *in* T.J. Givnish and K.J. Sytsma, eds. Molecular evolution and adaptive radiation. Cambridge Univ. Press, Cambridge, MA.

Thompson, C. E., E. B. Taylor, and J. D. McPhail. 1997. Parallel evolution of lake-stream pairs of threespine sticklebacks (*Gasterosteus*) inferred from mitochondrial DNA variation. Evolution 51:1955–1965.

Walker, J. A. 1997. Ecological morphology of lacustrine threespine stickleback *Gasterosteus aculeatus* L. (Gasterosteidae) body shape. Biol. J. Linn. Soc. 61:3–50.

Walker, J. A., and M. A. Bell. 2000. Net evolutionary trajectories of body shape evolution within a microgeographic radiation of threespine sticklebacks (*Gasterosteus aculeatus*). J. Zool. 252:293–302.

Walsh, B., and M. W. Blows. 2009. Abundant genetic variation plus strong selection = multivariate genetic constraints: a geometric view of adaptation. Annu. Rev. Ecol. Evol. S. 40:41–59.

Watanabe, K., S. Mori, and M. Nishida. 2003. Genetic relationships and origin of two geographic groups of the freshwater threespine stickleback, 'Hariyo'. Zool. Sci. 20:265–274.

Willacker, J.J., F.A. von Hippel, P.R. Wilton, and K.M. Walton. 2010. Classification of threespine stickleback along the benthic-limnetic axis. Biol. J. Linn. Soc. 101:595–608.

Zelditch, M. L., D. L. Swiderski, H. D. Sheets, and W. L. Fink. 2004. Geometric morphometrics for biologists: a primer. Elsevier Academic Press, London.

Zeng, Z.B. 1988. Long-term correlated response, interpopulation covariation, and interspecific allometry. Evolution 42: 363–374.

Associate Editor: L. Delph

Supporting Information

The following supporting information is available for this article:

Figure S1. The two major canonical variate axes (CV1 and CV2) of shape variation among populations within each geographical region in our study..
Figure S2. Opercle shape changes associated with divergence toward the freshwater morph in each region of our study.
Table S1. Parameters for the MANOVA (Table 2 in the main text).

Supporting Information may be found in the online version of this article.

Please note: Wiley-Blackwell is not responsible for the content or functionality of any supporting information supplied by the authors. Any queries (other than missing material) should be directed to the corresponding author for the article.